

# Top-quark spin correlation at Linear Colliders with anomalous couplings

Z.-H. Lin<sup>1</sup>, T. Han<sup>2</sup>, T. Huang<sup>1</sup>, J.-X. Wang<sup>1</sup> and X. Zhang<sup>1</sup>

<sup>1</sup>Institute of High Energy Physics, Academia Sinica,  
Beijing, 100039, P. R. China,

<sup>2</sup>Department of Physics, University of Wisconsin, Madison, WI 53706, USA

## Abstract

We investigate the feasibility of probing anomalous top-quark couplings of  $Wtb$ ,  $Zt\bar{t}$ , and  $\gamma t\bar{t}$  in terms of an effective Lagrangian with dimension-six operators at future  $e^+e^-$  linear colliders with a c. m. energy  $\sqrt{s} \sim 500 - 800$  GeV. We first examine the constraints on these anomalous couplings from the  $Z \rightarrow b\bar{b}$  data at LEP I and from unitarity considerations. We then consider in detail the effects of anomalous couplings on  $t\bar{t}$  spin correlations in the top-pair production and decay with three spin bases: the helicity, beamline and off-diagonal bases. Our results show that the polarized beams are more suitable for exploring the effects of different new operators. For polarized beams, the helicity basis yields the best sensitivity.

# 1 Introduction

The top-quark physics is one of the most important topics at a next generation linear collider. Near and above the threshold of a top quark and anti-top quark ( $t\bar{t}$ ), there will be about  $500 - 1000$   $t\bar{t}$  pairs produced per one  $\text{fb}^{-1}$  of integrated luminosity. Thus a high luminosity linear collider may allow for a good determination [1] of the top-quark mass ( $m_t$ ), its total width, the strong coupling constant  $\alpha_s$ , and even new physics effects such as from a virtual Higgs boson. Indeed, as the heaviest particle observed so far with a mass at the electroweak scale, the top quark may hold the key to new physics in the electroweak sector [2].

Without knowing the underlying dynamics beyond the standard model (SM), it is appropriate to parameterize new physics effects at low energies by an effective Lagrangian

$$\mathcal{L}_{eff} = \mathcal{L}_0 + \frac{1}{\Lambda^2} \sum_i C_i O_i + \mathcal{O}(\frac{1}{\Lambda^4}), \quad (1)$$

where  $\Lambda$  is a cutoff scale above which new physics sets in, and  $\mathcal{L}_0$  is the SM Lagrangian,  $O_i$  the SM-gauge-invariant dimension-six operators.  $C_i$  represent the coupling strengths of  $O_i$  [3]. In this paper we study the possibility of probing for anomalous top-quark couplings  $\gamma t\bar{t}$ ,  $Z t\bar{t}$  and  $W t b$  at Next Linear Colliders.

It has been shown in the literature that angular distribution in top-quark events at  $e^+e^-$  colliders bring useful information on the top-quark couplings, with which one can constrain its deviations from the SM [4, 5]. At  $e^+e^-$  colliders the top-quark pair is produced in a unique spin configuration, and the electroweak decay products of polarized top quark are strongly correlated to the spin axis. Parke and Shadmi [6] suggested several spin basis (helicity, beamline and off-diagonal basis) to discuss the  $t\bar{t}$  spin correlation. On the other hand, deviations from the SM may be observable via the top-quark spin correlations which depend sensitively on the couplings  $\gamma t\bar{t}$ ,  $Z t\bar{t}$  and  $W t b$ . The purpose of the current study is to explore which spin basis described in Ref. [6] is more suitable for studying a given anomalous top-quark coupling than others.

This paper is organized as follows. In section 2, we briefly review on effective lagrangian and present explicitly the dimension-6 operators which describe the anomalous couplings  $\gamma t\bar{t}$ ,  $Z t\bar{t}$  and  $W t b$ , then we examine the constraints on the coefficients of these operators. In section 3, we present a detail calculation of the top-quark spin correlation, and finally section 4 is summary and conclusion.

## 2 Effective interactions with top-quark

In the linearly realized effective Lagrangian [3], the anomalous top-quark couplings are described by higher dimensional operators. Recently the dimension-six operators involving the top quark and invariant under the SM gauge group were reclassified and some are analyzed in Refs. [7, 8]. Here we list all eleven dimension-six CP-even operators in Refs. [7, 8] which generate anomalous couplings of  $Z, \gamma, W^\pm$  to the top quark beyond the SM interactions,

$$O_{\Phi q}^{(1)} = i \left[ \Phi^\dagger D_\mu \Phi - (D_\mu \Phi)^\dagger \Phi \right] \bar{q}_L \gamma^\mu q_L,$$

$$\begin{aligned}
O_{\Phi q}^{(3)} &= i \left[ \Phi^\dagger \tau^I D_\mu \Phi - (D_\mu \Phi)^\dagger \tau^I \Phi \right] \bar{q}_L \gamma^\mu \tau^I q_L, \\
O_{Db} &= (\bar{q}_L D_\mu b_R) D^\mu \Phi + (D^\mu \Phi)^\dagger (\overline{D_\mu b_R q_L}), \\
O_{bW\Phi} &= \left[ (\bar{q}_L \sigma^{\mu\nu} \tau^I b_R) \Phi + \Phi^\dagger (\bar{b}_R \sigma^{\mu\nu} \tau^I q_L) \right] W_{\mu\nu}^I, \\
O_{qB} &= \left[ \bar{q}_L \gamma^\mu D^\nu q_L + \overline{D^\nu q_L} \gamma^\mu q_L \right] B_{\mu\nu}, \\
O_{qW} &= \left[ \bar{q}_L \gamma^\mu \tau^I D^\nu q_L + \overline{D^\nu q_L} \gamma^\mu \tau^I q_L \right] W_{\mu\nu}^I, \\
O_{t2} &= i \left[ \Phi^\dagger D_\mu \Phi - (D_\mu \Phi)^\dagger \Phi \right] \bar{t}_R \gamma^\mu t_R, \\
O_{Dt} &= (\bar{q}_L D_\mu t_R) D^\mu \tilde{\Phi} + (D^\mu \tilde{\Phi})^\dagger (\overline{D_\mu t_R q_L}), \\
O_{tB\Phi} &= \left[ (\bar{q}_L \sigma^{\mu\nu} t_R) \tilde{\Phi} + \tilde{\Phi}^\dagger (\bar{t}_R \sigma^{\mu\nu} q_L) \right] B_{\mu\nu}, \\
O_{tW\Phi} &= \left[ (\bar{q}_L \sigma^{\mu\nu} \tau^I t_R) \tilde{\Phi} + \tilde{\Phi}^\dagger (\bar{t}_R \sigma^{\mu\nu} \tau^I q_L) \right] W_{\mu\nu}^I, \\
O_{tB} &= \left[ \bar{t}_R \gamma^\mu D^\nu t_R + \overline{D^\nu t_R} \gamma^\mu t_R \right] B_{\mu\nu},
\end{aligned} \tag{2}$$

where  $\Phi$  is the Higgs doublet,  $\tilde{\Phi} = i\tau^2 \Phi^*$ ,  $\bar{q}_L = (\bar{t}_L, \bar{b}_L)$  and  $\tau^I$  are Pauli matrices. In Eq.(2), some of the operators induce energy-dependent couplings, some do not. If an anomalous coupling is function of energy, its effects on the physical quantity at different energy scale will be enhanced at high energy. In Table 1 we show explicitly the energy dependence of various couplings.

Now we present the experimental constraints on various operators. The most direct bounds on these operators come from the measurement of the observables  $R_b$  and  $A_{FB}^b$  at LEP. Updating the bounds in our previous paper Ref. [9] and assuming no accidental cancellation happens between different operators, as is often assumed, we give the limits below on each of operators in Eq. (2) at the  $1\sigma$  ( $3\sigma$ ) level as

$$\begin{aligned}
-1 \times 10^{-2} \text{ } (-2 \times 10^{-2}) &< \frac{v^2}{\Lambda^2} C_{qW} < -1 \times 10^{-4} \text{ } (1 \times 10^{-2}), \\
-2 \times 10^{-2} \text{ } (-5 \times 10^{-2}) &< \frac{v^2}{\Lambda^2} C_{qB} < -3 \times 10^{-4} \text{ } (2 \times 10^{-2}), \\
5 \times 10^{-5} \text{ } (-4 \times 10^{-3}) &< \frac{v^2}{\Lambda^2} C_{\Phi q}^{(1)} < 4 \times 10^{-3} \text{ } (8 \times 10^{-3}), \\
5 \times 10^{-5} \text{ } (-4 \times 10^{-3}) &< \frac{v^2}{\Lambda^2} C_{\Phi q}^{(3)} < 4 \times 10^{-3} \text{ } (8 \times 10^{-3}),
\end{aligned} \tag{3}$$

where  $v = 246$  GeV is the vacuum expectation value of the Higgs field. One can see that the constraints on some of the operators listed in Table 1 are relatively poor and there is room for possible new physics. However if the operators are not independent for a given model, cancellations may happen among different contributions, therefore the bounds obtained from  $R_b$  and  $A_{FB}^b$  may not be as restrictive [10].

Operators  $O_{t2}$ ,  $O_{Dt}$ ,  $O_{tW\Phi}$ ,  $O_{tB\Phi}$  and  $O_{tB}$ , are not constrained by  $R_b$  at tree level. However, at one-loop level they contribute to gauge boson self-energies. The authors of Ref. [8] have considered these constraints and showed some rather loose bounds on them. One can also put limits on various coefficients of the operators using the argument of partial wave

	$Zb\bar{b}$	$Wt\bar{b}$	$Zt\bar{t}$	$\gamma t\bar{t}$
SM	1	1	1	1
$O_{\Phi q}^{(1)}$	1		1	
$O_{\Phi q}^{(3)}$	1	1	1	
$O_{Db}$	$E/v$	$E/v$		
$O_{bW\Phi}$	$E/v$	$E/v$		
$O_{qB}$	$E^2/v^2$		$E^2/v^2$	$E^2/v^2$
$O_{qW}$	$E^2/v^2$	$E^2/v^2$	$E^2/v^2$	$E^2/v^2$
$O_{t2}$			1	
$O_{Dt}$		$E/v$	$E/v$	
$O_{tB\Phi}$			$E/v$	$E/v$
$O_{tW\Phi}$		$E/v$	$E/v$	$E/v$
$O_{tB}$			$E^2/v^2$	$E^2/v^2$

Table 1: The energy-dependence of dimension-six operators in Eq. (2) for couplings  $Zb\bar{b}$ ,  $Wt\bar{b}$ ,  $Zt\bar{t}$  and  $\gamma t\bar{t}$ . An overall normalization  $v^2/\Lambda^2$  has been factored out.

unitarity. The upper bounds are obtained for  $\Lambda \approx 3 - 1$  TeV in Ref. [8, 9]

$$\begin{aligned}
|C_{t2}| \frac{v^2}{\Lambda^2} &\simeq 0.29 - 2.6, \\
|C_{Dt}| \frac{v^2}{\Lambda^2} &\simeq 0.07 - 0.63 \quad \text{or} \quad |C_{Dt}| \frac{v^2}{\Lambda^2} \simeq -(0.04 - 0.40), \\
|C_{tW\Phi}| \frac{v^2}{\Lambda^2} &\simeq 0.02 - 0.15, \quad |C_{tB\Phi}| \frac{v^2}{\Lambda^2} \simeq 0.02 - 0.15, \\
|C_{tB}| \frac{v^2}{\Lambda^2} &\simeq 0.04 - 0.34 \quad \text{or} \quad |C_{tB}| \frac{v^2}{\Lambda^2} \simeq -(0.03 - 0.29).
\end{aligned} \tag{4}$$

Bounds on  $C_{Db}$  and  $C_{bW\Phi}$  are very weak due to their small contributions to  $Z \rightarrow b\bar{b}$  decay.

### 3 Top-quark spin correlation at linear colliders with anomalous couplings

We study in this section the production and decay of top-quark pair in the presence of anomalous couplings and examine the different behavior of top-quark spin correlations in various spin bases.

#### 3.1 The spin configuration in $t\bar{t}$ production

We consider the top-quark pair production in  $e^+e^-$  collisions

$$e^+e^- \rightarrow V^* \rightarrow t\bar{t}, \quad V = \gamma, Z. \quad (5)$$

To make our discussion general we write the effective CP-even vertices of  $Zt\bar{t}$  and  $\gamma t\bar{t}$  as

$$\Gamma_{Vt\bar{t}}^\mu = ieQ_{tR}^V \gamma^\mu P_R + ieQ_{tL}^V \gamma^\mu P_L + ieQ_{t\bar{t}}^V \frac{(p_t - p_{\bar{t}})^\mu}{m_t}, \quad (6)$$

where  $P_{L,R}$  are the projection operators  $(1 \mp \gamma_5)/2$  and  $p_t$  and  $p_{\bar{t}}$  are the momenta of the outgoing top quark and top antiquark, respectively. We have neglected the terms which contain  $k^\mu = (p_t + p_{\bar{t}})^\mu$  by using the Dirac equation for massless electrons. In terms of the gauge-invariant operators in Eq. (2), the left(right)-handed couplings  $Q_{tL}^V(Q_{tR}^V)$  and the electroweak magnetic-moment couplings  $Q_{t\bar{t}}^V$  are

$$\begin{aligned} Q_{tR}^\gamma &= Q_t \left( 1 - \frac{C_{tB} c_W k^2}{\Lambda^2 e Q_t} + \frac{C_{tW\phi} s_W + C_{tB\phi} c_W}{\Lambda^2} \frac{8}{\sqrt{2}} \frac{m_W m_t}{ge Q_t} \right), \\ Q_{tL}^\gamma &= Q_t \left( 1 - \frac{C_{qW} s_W + C_{qB} c_W}{\Lambda^2} \frac{k^2}{e Q_t} + \frac{C_{tW\phi} s_W + C_{tB\phi} c_W}{\Lambda^2} \frac{8}{\sqrt{2}} \frac{m_W m_t}{ge Q_t} \right), \\ Q_{tR}^Z &= Q_t^R \left( 1 + \frac{C_{tB} s_W k^2}{\Lambda^2 e Q_t^R} - \frac{C_{t2} m_Z v}{\Lambda^2 e Q_t^R} + \frac{C_{tW\phi} c_W - C_{tB\phi} s_W}{\Lambda^2} \frac{8}{\sqrt{2}} \frac{m_W m_t}{ge Q_t^R} \right), \\ Q_{tL}^Z &= Q_t^L \left( 1 - \frac{C_{qW} c_W - C_{qB} s_W}{\Lambda^2} \frac{k^2}{e Q_t^L} - \frac{C_{\phi q}^{(1)} - C_{\phi q}^{(3)}}{\Lambda^2} \frac{m_Z v}{e Q_t^L} \right. \\ &\quad \left. + \frac{C_{tW\phi} c_W - C_{tB\phi} s_W}{\Lambda^2} \frac{8}{\sqrt{2}} \frac{m_W m_t}{ge Q_t^L} \right), \\ Q_{t\bar{t}}^\gamma &= -\frac{C_{tW\phi} s_W + C_{tB\phi} c_W}{\Lambda^2} \frac{4}{\sqrt{2}} \frac{m_W m_t}{ge}, \\ Q_{t\bar{t}}^Z &= -\frac{C_{tW\phi} c_W - C_{tB\phi} s_W}{\Lambda^2} \frac{4}{\sqrt{2}} \frac{m_W m_t}{ge} + \frac{C_{Dt}}{\Lambda^2} \frac{m_Z m_t}{2\sqrt{2}e}, \end{aligned} \quad (7)$$

where  $Q_e = -1$ ,  $Q_t = \frac{2}{3}$ ,  $Q_{eR} = \frac{s_W}{c_W}$ ,  $Q_{eL} = \frac{2s_W^2 - 1}{2s_W c_W}$ ,  $Q_t^R = -\frac{2s_W}{3c_W}$  and  $Q_t^L = \frac{3 - 4s_W^2}{6s_W c_W}$ , which are the SM couplings.

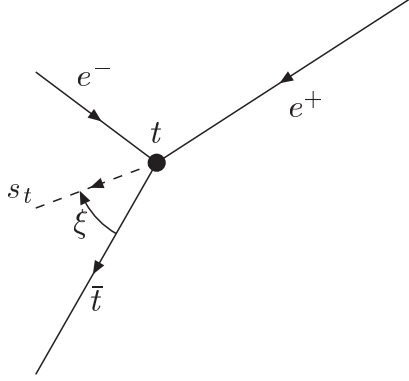


Figure 1: The spin axis  $\vec{s}_t$  defined in the top-quark rest-frame with respect to the anti-top momentum direction.

The discussion on the polarized top-quark production requires a definite spin basis. In the SM, it is shown that the size of top-spin correlation for different spin bases are quite distinct [6, 11, 12]. In the presence of anomalous couplings, we adopt the same notation of generic spin basis [6]. A general spin axis  $\vec{s}_t$  for the top quark is defined by an angle  $\xi$  (clockwise) in the  $t$  rest-frame with respect to  $\vec{p}_{\bar{t}}$  direction, as shown in Fig. 1. The top antiquark spin axis can be defined with the same angle  $\xi$ , but in the  $\bar{t}$  rest-frame with respect to  $\vec{p}_t$  direction. For instance, a polarized state  $t_{\uparrow}\bar{t}_{\uparrow}$  refers to a top quark with spin along  $+\vec{s}_t$  and an anti-top quark with spin along  $+\vec{s}_{\bar{t}}$ . With this choice of spin basis, the tree level differential polarized cross sections are given in terms of the center-of-mass energy  $\sqrt{s}$  and top-quark speed  $\beta = \sqrt{1 - 4m_t^2/s}$  as

$$\begin{aligned}
\frac{d\sigma(e_L^- e_R^+ \rightarrow t_{\uparrow}\bar{t}_{\uparrow})}{d\cos\theta} &= \frac{d\sigma(e_L^- e_R^+ \rightarrow t_{\downarrow}\bar{t}_{\downarrow})}{d\cos\theta} \\
&= \left(\frac{3\pi\alpha^2}{2s}\beta\right) |A_{LR}\cos\xi - B_{LR}\sin\xi - 2f_{tt}^L\gamma\beta^2\sin\theta\cos\xi|^2, \\
\frac{d\sigma(e_L^- e_R^+ \rightarrow t_{\uparrow}\bar{t}_{\downarrow})}{d\cos\theta} &= \frac{d\sigma(e_L^- e_R^+ \rightarrow t_{\downarrow}\bar{t}_{\uparrow})}{d\cos\theta} \\
&= \left(\frac{3\pi\alpha^2}{2s}\beta\right) |A_{LR}\sin\xi + B_{LR}\cos\xi \pm D_{LR} - 2f_{tt}^L\gamma\beta^2\sin\theta\sin\xi|^2, \quad (8)
\end{aligned}$$

where  $\theta$  is the top scattering angle with respect to the  $e^-$  beam and  $\gamma = 1/\sqrt{1 - \beta^2}$ , and

$$\begin{aligned}
A_{LR} &= [(f_{LL} + f_{LR})\sqrt{1 - \beta^2}\sin\theta]/2, \\
B_{LR} &= [f_{LL}(\cos\theta + \beta) + f_{LR}(\cos\theta - \beta)]/2, \\
D_{LR} &= [f_{LL}(1 + \beta\cos\theta) + f_{LR}(1 - \beta\cos\theta)]/2, \quad (9)
\end{aligned}$$

with

$$f_{IJ} = Q_e Q_{tIJ}^\gamma + Q_{eI} Q_{tJ}^Z \frac{s}{s - m_Z^2 + im_Z \Gamma_Z}, \quad I, J = R, L,$$

$$f_{t\bar{t}}^I = Q_e Q_{t\bar{t}}^\gamma + Q_{eI} Q_{t\bar{t}}^Z \frac{s}{s - m_Z^2 + im_Z \Gamma_Z}, \quad I = R, L. \quad (10)$$

Similarly, one can obtain the differential cross sections for a different beam polarization  $e_R^- e_L^+$  by interchanging the labels  $R \leftrightarrow L$  and  $\uparrow \leftrightarrow \downarrow$  in Eq. (8).

There are three typical bases characterized by choosing a different angle  $\xi$  as follows.

- Helicity basis: For  $\cos \xi = +1$  ( $-1$ ), the top-quark spin axis is against (along) its direction of motion.
- Beamline basis: For  $\cos \xi = (\cos \theta + \beta)/(1 + \beta \cos \theta)$ , the top-quark spin is in the positron direction in the top rest-frame.
- Off-diagonal basis:  $\tan \xi = A_{LR}^{SM}/B_{LR}^{SM}$ , where  $A_{LR}^{SM}$  and  $B_{LR}^{SM}$  represent the SM parts of  $A_{LR}$  and  $B_{LR}$  respectively in Eq. (9). Although one can similarly define another off-diagonal basis for  $e_R^- e_L^+$  scattering, the considerably small difference between the two bases allows us to use the off-diagonal basis for  $e_L^- e_R^+$  even when discussing  $e_R^- e_L^+$  scattering [6].

Regarding the off-diagonal basis, Parke and collaborators have applied it to top-pair production at a linear and hadron colliders [6, 12], and found many advantages in studying physics of the top quark. It gives rise to substantial spin correlation than the helicity or beamline basis do [14]. For example,  $\frac{d\sigma}{d\cos\theta}(e_L^- e_R^+ \rightarrow t_\uparrow \bar{t}_\uparrow)$  and  $\frac{d\sigma}{d\cos\theta}(e_L^- e_R^+ \rightarrow t_\downarrow \bar{t}_\downarrow)$  are equal to zero for off-diagonal basis at the SM tree level and therefore all  $t\bar{t}$  pairs are of opposite spins. Moreover, the dominant component up to 97% of the  $e_L^- e^+$  cross section is  $t_\uparrow \bar{t}_\downarrow$  at the energy  $\sqrt{s} = 400$  GeV, much larger than 58% in the helicity basis [6]. Furthermore, the top-pair production density matrix in the off-diagonal basis is greatly simplified due to many zero entries in the matrix [12].

In the presence of anomalous couplings, however, the situation may be different due to the very different helicity structures of the new operators. Thus we will consider all of the three bases in the following discussions in order to find out which basis is more sensitive to which class of operators. Of the eleven operators listed in Eq. (2) we will take two operators  $O_{tB}$  and  $O_{tW\phi}$  for a detail study. We choose these two operators for the following reasons. First, they have distinctive energy-dependence as seen in Table 1, which characterizes a typical feature of anomalous couplings. Second, while the operator  $O_{tB}$  modifies  $Zt\bar{t}$  and  $\gamma t\bar{t}$  which affect the top-quark production, the operator  $O_{tW\phi}$  modifies the top-quark decay as well. In addition, these two operators have no direct effects on  $Z \rightarrow b\bar{b}$  measurement, so their coefficients are not strongly constrained. Consequently, the top-quark production and decay would be the unique place to explore them if they generate sizeable effects at high energy experiments. Numerically taking the conservative limits in Eq. (4), we will adopt

$$|C_{tB}| \frac{v^2}{\Lambda^2}, \quad |C_{tW\phi}| \frac{v^2}{\Lambda^2} < 0.02, \quad (11)$$

in our analysis.

We plot in Fig. 2 the total cross section and various polarized cross sections of  $e^+e^- \rightarrow t\bar{t}$  versus  $\sqrt{s}$  in the presence of operators  $O_{tB}$  and  $O_{tW\phi}$ . One can clearly see from the figure the effects of new physics. However, the operator  $O_{tW\phi}$  seems not to make any correction to  $\sigma(e_R^- e^+)$ . This is due to the fact that the couplings of the right-handed electron with  $\gamma$  and  $Z$  are from  $U_Y(1)$  gauge interaction, while  $O_{tW\phi}$  are of purely  $SU_L(2)$  interactions. We have numerically verified the cancellation of  $O_{tW\phi}$  between  $e_R^- e^+ \rightarrow \gamma^* \rightarrow t\bar{t}$  and  $e_R^- e^+ \rightarrow Z^* \rightarrow t\bar{t}$  contributions.

In Fig. 3 and Fig. 4, we plot the energy dependence of the fraction of top quark pair production in three different bases for  $O_{tB}$  and  $O_{tW\phi}$ , respectively. The fraction is defined by  $\sigma(e_{L/R}^- e^+ \rightarrow t_{s_t} \bar{t}_{s_{\bar{t}}})/\sigma_{total}$ , where  $\sigma_{total}$  is the polarized total cross section for the process  $e_{L/R}^- e^+ \rightarrow t_{s_t} \bar{t}_{s_{\bar{t}}}$  including appropriate anomalous couplings. While the off-diagonal, beamline, and helicity bases present the most, medium, and least polarization of  $t\bar{t}$  states, respectively, the percentage effects due to new operators are of reversed order, namely it is the most significant in the helicity basis instead. The reason is as follows: The new physics effects come dominantly from the interference terms between the SM and anomalous couplings at the order of  $1/\Lambda^2$ , and the pure contributions of the anomalous couplings set in at a higher order of  $1/\Lambda^4$ . Since in the SM with the off-diagonal basis, the spin configuration is almost exclusively  $t_{\uparrow} \bar{t}_{\downarrow}$ , the leading anomalous contribution coming from the interference is forced to be in the same unique configuration. On the other hand, the helicity basis presents a large partition between  $t_{\uparrow} \bar{t}_{\downarrow}$  and  $t_{\downarrow} \bar{t}_{\uparrow}$ , so that it allows a more significant effect in reshuffling these two configurations due to the existence of the anomalous operators, thus leading to possibly appreciable differences when comparing with the SM predictions. We notice that because of the strong energy dependence of the couplings, the effects are generally larger at higher energies. Moreover, we also observed a particularly large deviation from the SM prediction for the operator  $O_{tB}$  in  $e_R^- e_L^+$  reaction near  $\sqrt{s} \approx 850$  GeV, see Fig. 3. This is due to the corrections from the direct term which is proportion to  $C_{tB}^2 \times \frac{s^2}{\Lambda^4}$ . In the case the interference term gives the negative contributions and the direct term gives the positive contributions, there should be a peak at some energy scale and this scale is decided by the size of  $C_{tB}$  and  $\Lambda$ . For the parameter we selected i.e.  $C_{tB} v^2/\Lambda^2 = 0.02$ , it appears at the energy of 850 GeV.

In Fig. 5 and Fig. 6, we show the behavior of the fraction at  $\sqrt{s} = 800$  GeV as a function of the couplings  $O_{tB}$  and  $O_{tW\phi}$ , respectively. The SM prediction can be read off from the figures for the couplings to be zero. The sign of the coupling  $O_{tB}$  may be inferred by different beam polarization choices. For instance, consider a  $t_{\uparrow} \bar{t}_{\uparrow}$  final state as in Fig. 5, a positive coupling gives significant enhancement to  $e_L^- e_R^+$  initial state and a negative coupling leads a reduction for  $e_R^- e_L^+$  initial state.

Given the discussion above, we conclude that the percentage corrections from anomalous couplings to the spin configuration in the off-diagonal basis are much smaller than that in the helicity basis for the polarized  $e^- e^+$  scattering. The enhanced spin correlation in the SM is not necessarily beneficial in distinguishing contributions from anomalous couplings.



### 3.2 The effects on the correlation coefficient in top-quark decay

We now consider the process of top decay and examine the effects of anomalous couplings  $Wtb$  on the correlation coefficient. In general the effective vertex of  $Wtb$  coupling can be written as

$$\Gamma_{tb}^\mu = i\frac{1}{\sqrt{2}}[g_L\gamma^\mu P_L + g_R\gamma^\mu P_R + g_{tb}^L\frac{(p_t + p_b)^\mu}{m_t}P_L + g_{tb}^R\frac{(p_t + p_b)^\mu}{m_t}P_R], \quad (12)$$

where  $p_t$  and  $p_b$  are the momenta of incoming top quark and outgoing bottom quark respectively and

$$\begin{aligned} g_L &= gV_{tb} - \frac{C_{qW}}{\Lambda^2}(2k^2) + \frac{C_{\phi q}^{(3)}}{\Lambda^2}\frac{4m_W^2}{g} + \frac{C_{tW\phi}}{\Lambda^2}\frac{8m_W m_t}{\sqrt{2}}, \\ g_R &= \frac{C_{bW\phi}}{\Lambda^2}\frac{8m_W m_t}{\sqrt{2}g} + \frac{C_{t3}}{\Lambda^2}\frac{2m_W^2}{g}, \\ g_{tb}^L &= -\frac{C_{bW\phi}}{\Lambda^2}\frac{8m_W m_t}{\sqrt{2}g} - \frac{C_{Db}}{\Lambda^2}\frac{m_W m_t}{\sqrt{2}}, \\ g_{tb}^R &= -\frac{C_{tW\phi}}{\Lambda^2}\frac{8m_W m_t}{\sqrt{2}g} - \frac{C_{Dt}}{\Lambda^2}\frac{m_W m_t}{\sqrt{2}}. \end{aligned} \quad (13)$$

Note that the SM coupling is the first term in  $g_L$ . It is easy to see from Eq. (12) that the leading corrections to the top decay at order  $1/\Lambda^2$  come from interference between the SM and terms in  $g_L$  and terms in  $g_{tb}^R$ . We will henceforth neglect effects from  $g_R$  and  $g_{tb}^L$  which are suppressed by  $1/\Lambda^4$ .

Using the narrow width approximation for the  $W$  boson

$$\frac{1}{(k^2 - m^2)^2 + m^2\Gamma^2} \rightarrow \frac{\pi}{m\Gamma}\delta(k^2 - m^2), \quad (14)$$

we express the polarized differential top-decay width for  $t \rightarrow bf\bar{f}'$  as

$$\begin{aligned} \frac{d\Gamma(t_\uparrow \text{ or } t_\downarrow)}{d\cos\theta_D} &= \frac{m_t}{16(4\pi)^2} \frac{g^2}{\bar{y}} \frac{\pi g_L^2}{\Gamma_W/m_W} \frac{1}{6}(1 - \bar{y})^2(1 + 2\bar{y})(1 + \frac{2g_{tb}^R}{g_L} \frac{1 - \bar{y}}{1 + 2\bar{y}})(1 \pm \cos\theta_D) \\ &\quad + \mathcal{O}(\frac{1}{\Lambda^4}), \end{aligned} \quad (15)$$

where  $\bar{y} = m_W^2/m_t^2$  and  $\theta_D$  is the angle between the momentum direction of the lepton or down-type light quark and the top-spin axis in the top-quark rest-frame. Here, we neglect all fermion mass except top quark. The polarized differential decay rate in the SM is conveniently parameterized as

$$\frac{1}{\Gamma} \frac{d\Gamma}{d\cos\theta_i} = \frac{1 \pm \alpha_i \cos\theta_i}{2} \quad (16)$$

	$\Gamma$ [GeV]
SM ( $C_i = 0$ )	0.178
$C_{qW}v^2/\Lambda^2 = 0.02$	0.177
$C_{qW}v^2/\Lambda^2 = -0.02$	0.180
$C_{tW\phi}v^2/\Lambda^2 = 0.02$	0.188
$C_{tW\phi}v^2/\Lambda^2 = -0.02$	0.169
$C_{Dt}v^2/\Lambda^2 = 0.02$	0.177
$C_{Dt}v^2/\Lambda^2 = -0.02$	0.179

Table 2: The leptonic decay width ( $t \rightarrow W^+b \rightarrow \bar{l}\nu b$ ) containing the contributions from the SM plus anomalous couplings.

where  $i = b, D$  (lepton or down-type light quark) or  $U$  (neutrino or up-type light quark). The correlation coefficients  $\alpha_i$  are 1,  $-0.31$  and  $-0.41$  for  $D, U$  and  $b$ , respectively [16].

Comparing Eq. (15) with Eq. (16), we find that the anomalous couplings do not give corrections to the correlation coefficient  $\alpha_D$  up to  $\mathcal{O}(\frac{1}{\Lambda^2})$ . Since all spin bases are defined in the process of top production, the angular distributions of different decay products give same relationship of different spin bases. Therefore we select the angle distribution between the momentum direction of the lepton or down-type light quark and the top-spin axis at top rest frame, whose correlation coefficient  $\alpha_D$  is largest. We will show in the next subsection that this selection is advantageous for us to define observables with large value.

We have also recalculated the top-decay width in the presence of the anomalous coupling, which is shown in Table 2. We find the corrections may be as large as 5%. It would be very interesting to determine the top width or individual branching fractions to this level of accuracy.

### 3.3 Spin asymmetry and spin-spin asymmetry

Since we need the construction of the full event kinematics for  $t\bar{t}$  decays, the dileptonic decay mode would be difficult to make use of due to the two missing neutrinos. Although the identification of six-jet events in the pure hardonic decay mode should be viable, it would be impossible to sort out quarks from anti-quarks in the four light jets. The semileptonic mode becomes the unique channel for the study of top-spin correlations. We consider the case where one lepton with positive charge comes from top-quark decay while two partons come from top antiquark decay. To obtain the differential cross section of  $e^-e^+ \rightarrow t\bar{t} \rightarrow (b\bar{l}\nu_l)(\bar{b}UD)$ , the production and decay spin density matrix are always used as the usual approach in the approximation of narrow widths for top quark and  $W$  boson [15, 16]. After integrating over

all azimuthal angles, one gets the double differential rate as

$$\frac{1}{\sigma} \frac{d^2\sigma}{d(\cos\theta_{\bar{l}})d(\cos\theta_D)} = \frac{1}{4}(1 + \langle s_t \rangle \alpha_{\bar{l}} \cos\theta_{\bar{l}} + \langle s_{\bar{t}} \rangle \alpha_D \cos\theta_D + \langle s_t s_{\bar{t}} \rangle \alpha_{\bar{l}} \alpha_D \cos\theta_{\bar{l}} \cos\theta_D)$$

where  $\bar{l}$  ( $D$ ) is the decay product of top quark (top antiquark) and  $\cos\theta_{\bar{l}}$  ( $\cos\theta_D$ ) is the angle defined in Eq (15).  $\langle s_t \rangle$ ,  $\langle s_{\bar{t}} \rangle$  and  $\langle s_t s_{\bar{t}} \rangle$  are  $t$ ,  $\bar{t}$  and  $t\bar{t}$  correlation functions, respectively. They can be expressed as

$$\begin{aligned} \langle s_t \rangle &= \sum_{I,J=L,R} (R(e_I^- e_J^+ \rightarrow t_{\uparrow} \bar{t}_{\uparrow}) + R(e_I^- e_J^+ \rightarrow t_{\uparrow} \bar{t}_{\downarrow}) - R(e_I^- e_J^+ \rightarrow t_{\downarrow} \bar{t}_{\uparrow}) - R(e_I^- e_J^+ \rightarrow t_{\downarrow} \bar{t}_{\downarrow})), \\ \langle s_{\bar{t}} \rangle &= \sum_{I,J=L,R} (R(e_I^- e_J^+ \rightarrow t_{\uparrow} \bar{t}_{\uparrow}) - R(e_I^- e_J^+ \rightarrow t_{\uparrow} \bar{t}_{\downarrow}) + R(e_I^- e_J^+ \rightarrow t_{\downarrow} \bar{t}_{\uparrow}) - R(e_I^- e_J^+ \rightarrow t_{\downarrow} \bar{t}_{\downarrow})), \\ \langle s_t s_{\bar{t}} \rangle &= \sum_{I,J=L,R} (R(e_I^- e_J^+ \rightarrow t_{\uparrow} \bar{t}_{\uparrow}) - R(e_I^- e_J^+ \rightarrow t_{\uparrow} \bar{t}_{\downarrow}) - R(e_I^- e_J^+ \rightarrow t_{\downarrow} \bar{t}_{\uparrow}) + R(e_I^- e_J^+ \rightarrow t_{\downarrow} \bar{t}_{\downarrow})). \end{aligned}$$

where

$$R(e_I^- e_J^+ \rightarrow t_{s_t} \bar{t}_{s_{\bar{t}}}) = \frac{\sigma(e_I^- e_J^+ \rightarrow t_{s_t} \bar{t}_{s_{\bar{t}}})}{\sigma_T}, \quad I, J = L, R \text{ and } s_t, s_{\bar{t}} = \uparrow, \downarrow. \quad (17)$$

Here,  $\sigma(e_I^- e_J^+ \rightarrow t_{s_t} \bar{t}_{s_{\bar{t}}})$  are the polarized cross section in top-pair production which could be obtained by integrating over  $\cos\theta$  in Eq. (8).  $\sigma_T$  is the total cross section of  $e^- e^+ \rightarrow t\bar{t}$ .

Integrating over  $\cos\theta_D$ , one obtains

$$\frac{1}{\sigma} \frac{d\sigma}{d(\cos\theta_{\bar{l}})} = \frac{1}{2}(1 + \alpha_{\bar{l}}^s \cos\theta_{\bar{l}}), \quad (18)$$

where the effective correlation coefficient  $\alpha_{\bar{l}}^s$  is given by

$$\alpha_{\bar{l}}^s = \langle s_t \rangle \alpha_{\bar{l}}. \quad (19)$$

Such effective spin correlation corresponds to the top-quark spin asymmetry which is some observable and can be derived as

$$A_s = \frac{N(\cos\theta_{\bar{l}} > 0) - N(\cos\theta_{\bar{l}} < 0)}{N(\cos\theta_{\bar{l}} > 0) + N(\cos\theta_{\bar{l}} < 0)} = \frac{\alpha_{\bar{l}}^s}{2}. \quad (20)$$

Similarly, we integrate over  $\cos\theta_D$  in the region of

$$0 < \cos\theta_D < 1 \quad (21)$$

and obtain

$$\left. \frac{1}{\sigma} \frac{d\sigma}{d(\cos\theta_{\bar{l}})} \right|_{\cos\theta_D > 0} \propto \frac{1}{2}(1 + \alpha_{\bar{l}}^{ss} \cos\theta_{\bar{l}}), \quad (22)$$

where

$$\alpha_{\bar{l}}^{ss} = \frac{2\langle s_{\bar{l}} \rangle + \langle s_t s_{\bar{l}} \rangle \alpha_D}{2 + \alpha_D \langle s_t \rangle} \alpha_{\bar{l}}. \quad (23)$$

This effective correlation coefficient corresponds to the spin-spin asymmetry which is defined as

$$A_{ss} = \frac{N(\cos \theta_{\bar{l}} > 0, \cos \theta_D > 0) - N(\cos \theta_{\bar{l}} < 0, \cos \theta_D > 0)}{N(\cos \theta_{\bar{l}} > 0, \cos \theta_D > 0) + N(\cos \theta_{\bar{l}} < 0, \cos \theta_D > 0)} = \frac{\alpha_{\bar{l}}^{ss}}{2}. \quad (24)$$

Even though distinction of the down-type quark and the up-type quark in the final decay state is impossible, we can at least hope to measure  $A_{ss}$  by a statistical method [17].

Eqs. (19) and (23) are generically valid for other decay product. One can simply replace  $\alpha_{\bar{l}}$  by  $\alpha_i$ , where  $i$  denotes any decay product. Therefore, the observables  $A_s$  and  $A_{ss}$  are proportional to the correlations coefficient  $\alpha_i$  and we choose the largest value  $\alpha_i = \alpha_{\bar{l}}$ .

The spin asymmetry  $A_s$  and spin-spin asymmetry  $A_{ss}$  are shown versus  $\sqrt{s}$  for  $O_{tB}$  in the case of right-hand polarized electron beam in Fig. 7, and for  $O_{tW\phi}$  in the case of left-hand polarized electron beam in Fig. 8. With the analysis in the last two subsections, it is not surprising to see that the corrections to  $A_s$  and  $A_{ss}$  are the most significant in the helicity basis for  $O_{tB}$  and  $O_{tW\phi}$ .

For the left-hand polarized electron beam, the top quark with up-spin is the dominant configuration and for the right-hand polarized electron beam the dominant one is that with down-spin. Due to the cancellation between different polarized beams, there is no unique basis which is optimal for searching new physics. In Fig. 9 and Fig. 10, we show the spin asymmetry  $A_s$  and spin-spin asymmetry  $A_{ss}$  versus  $\sqrt{s}$  for  $O_{tB}$  and  $O_{tW\phi}$  in the case of unpolarized beam. The corrections to  $A_s$  and  $A_{ss}$  are the most significant in the helicity basis for  $O_{tB}$  and in the off-diagonal basis for  $O_{tW\phi}$ , related to the chirality structure of the operators.

## 4 Summary and conclusion

We took an effective Lagrangian approach to new physics in the top-quark sector and discussed the anomalous-coupling effects on the spin correlation in top-quark pair production and decay. In the framework of the generic spin basis proposed by Parke and collaborators, we performed detail calculations of spin correlations, spin asymmetry and spin-spin asymmetry for three different bases. We found that the helicity basis is the best for polarized beam, and for unpolarized beam the optimal choice of the spin basis depends on the specific form of the new physics. Specifically the helicity basis will be the best choice in probing for new physics associated with  $U_Y(1)$  type operators such as  $O_{tB}$ , while the off-diagonal basis appears to be more suitable for  $SU_L(2)$  type operators such as  $O_{tW\phi}$ .

*Acknowledgments:* We thank E.L. Berger, K. Hagiwara, S. Parke and J.-M. Yang for discussions. T. Huang, Z.-H. Lin and X. Zhang were supported in part by the NSF of

China. T. Han was supported in part by a US DOE grant No. DE-FG02-95ER40896 and by Wisconsin Alumni Research Foundation.

## References

- [1] For a recent review, see *e. g.*, A.H. Hoang, in the proceedings of *Physics and Experiments with future Linear  $e^+e^-$  Colliders*, Sitges, Barcelona, Spain (1999), p. 69 [hep-ph/9909414].
- [2] R.D. Peccei and X. Zhang, Nucl. Phys. B337, 269 (1990); R.D. Peccei, S. Peris and X. Zhang, Nucl. Phys. B349, 305 (1991).
- [3] C. J. C. Burgess and H. J. Schnitzer, Nucl. Phys. **B228**, 454 (1983); C. N. Leung, S. T. Love and S. Rao, Z. Phys. **C31**, 433 (1986); W. Buchmuller and D. Wyler, Nucl. Phys. **B268**, 621 (1986); K. Hagiwara, S. Ishihara, R. Szalapski and D. Zeppenfeld, Phys. Rev. **D48**, 2182 (1993).
- [4] D. Atwood and A. Soni, Phys. Rev. **D45**, 2405 (1992); D. Atwood, A. Aeppli and A. Soni, Phys. Rev. Lett **69**, 2754 (1992); D. Atwood, S. Bar-Shalom, G. Eilam and A. Soni, Phys. Rept. **347**, 1 (2001); B. Holdom and T. Torma, Phys. Rev. **D60**, 114010 (1999); T. Torma, hep-ph/9912281; S.M. Lietti and H. Murayama, Phys. Rev. **D62**, 074003 (2000); E. Boos, M. Dubinin, M. Sachwitz, H.J. Schreiber, Eur. Phys. J. **C16**, 269 (2000); S.D. Rindani, hep-ph/0002006; B. Grzadkowski and Z. Hioki, hep-ph/0003294; Z. Hioki, hep-ph/0104105; S.D. Rindani, hep-ph/0105318.
- [5] Y. Kiyo, J. Kodaira, K. Morii, T. Nasuno and S. Parke, Nucl. Phys. Proc. Suppl. **89**, 37, (2000) ; Y. Kiyo, J. Kodaira and K. Morii, Eur.Phys.J.**C18**, 327, (2000).
- [6] S. Parke and Y. Shadmi, Phys. Lett. **B387**, 199 (1996).
- [7] K. Whisnant, J. M. Yang, B.-L. Young and X. Zhang, Phys. Rev. **D56**, 467 (1997).
- [8] G. J. Gounaris, D. T. Papadamou and F. M. Renard, Z. Phys. **C76**, 333 (1997).
- [9] T. Han, T.Huang, Z.-H. Lin, J.-X. Wang and X. Zhang, Phys. Rev. **D61**, 015006 (2000).
- [10] F. del Aguila, M. Perez-Victoria and J. Santiago Phys. Lett. **B492**, 98 (2000); JHEP **0009**, 011, (2000).
- [11] G. Mahlon and S. Parke, Phys. Rev. **D53**, 4886 (1995).
- [12] G. Mahlon and S. Parke, Phys. Lett. **B411**, 173 (1997).
- [13] T. Nasuno, hep-ph/9906252, *doctor thesis*.
- [14] J. Kodaira, T. Nasuno and S. Parke, Phys. Rev. **D59**, 014023 (1999).

- [15] S.Y. Choi, A. Djouadi, H. Dreiner, J. Kalinowski and P.M. Zerwas, Eur. Phys. J. **C7**, 123(1999); M.S. Baek, S.Y. Choi and C.S. Kim, Phys. Rev. **D56**, 6835 (1997).
- [16] J.H. Kühn, A. Reiter and P.M. Zerwas, Nucl. Phys. **B272**, 560 (1986); M. Jezabek and J.H. Kühn, *ibid.* **B320**, 20 (1989); A. Czarnecki, M. Jezabek and J.H. Kühn, *ibid.* **B427**, 3 (1994).
- [17] *Future Electro Weak Physics at the Fermilab Tevatron Report of the tev2000 Study Group*, FERMILAB-Pub-96/082, ed. by D. Amidei and R. Brock.

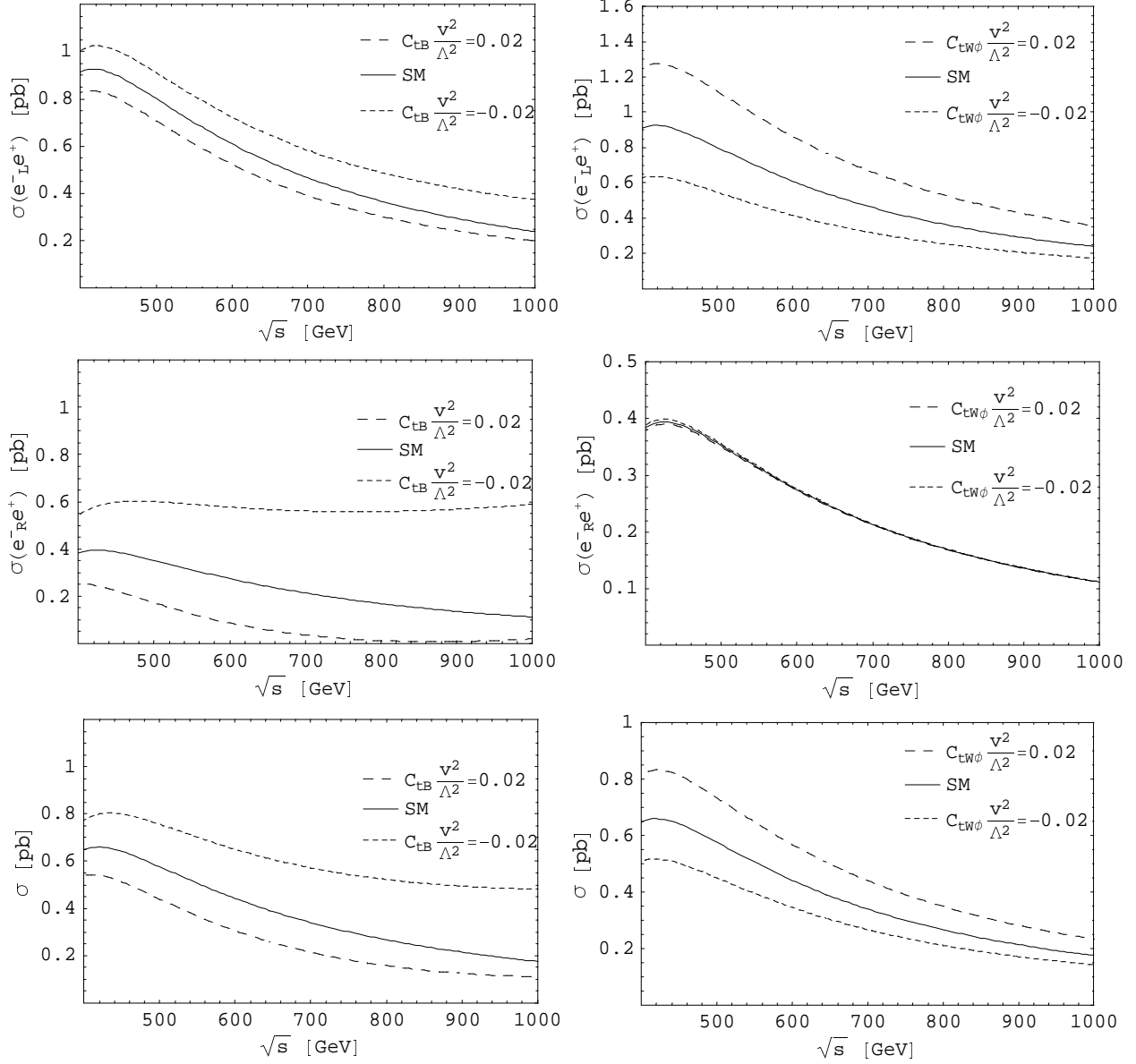


Figure 2: The total cross sections and polarized cross sections for  $e^+e^- \rightarrow t\bar{t}$  production versus the  $e^+e^-$  c. m. energy for  $O_{tB}$  and  $O_{tW\phi}$ . The solid curves are for the SM prediction.

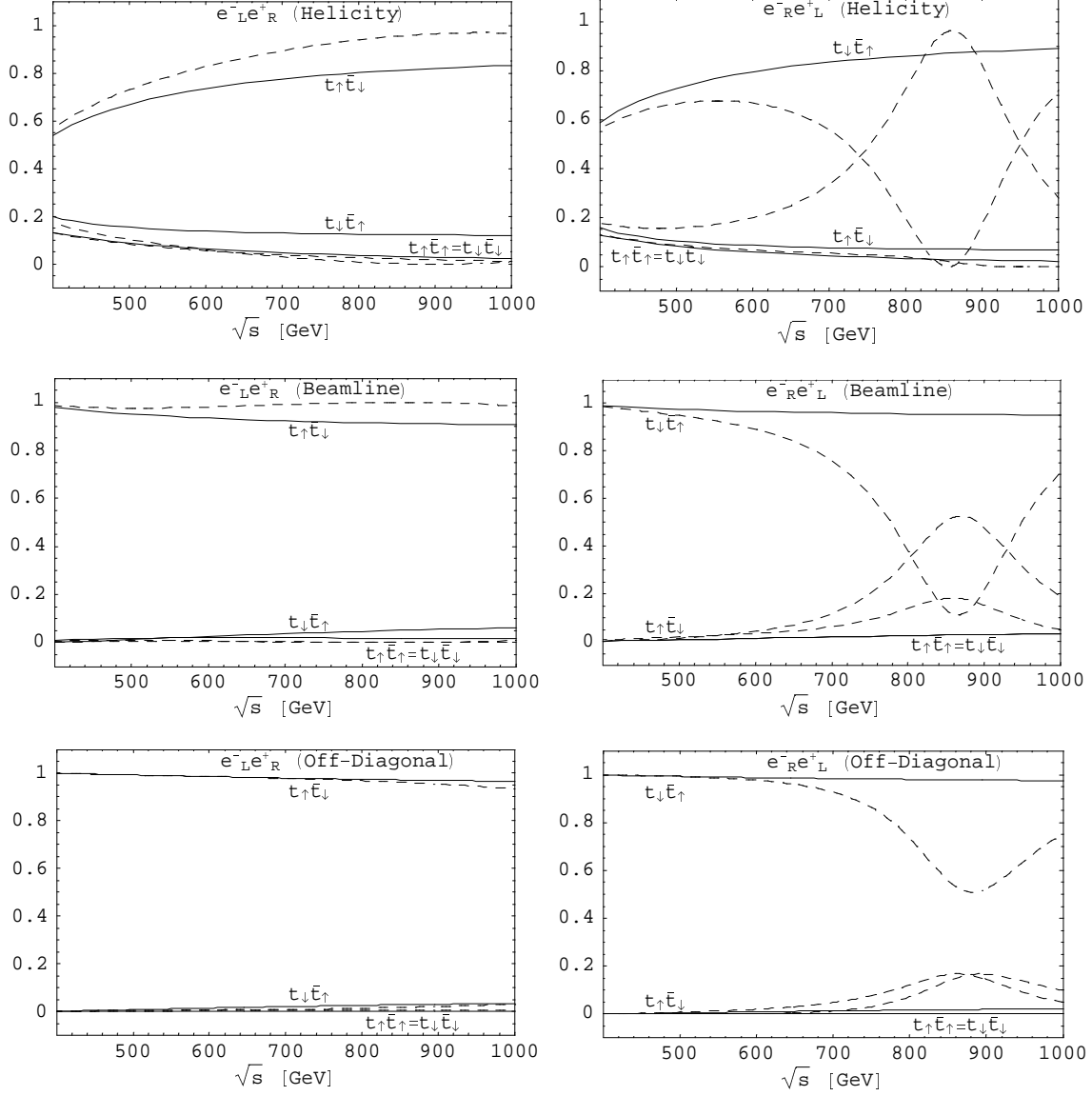


Figure 3: The fraction of top-quark pair production versus the  $e^+e^-$  c. m. energy  $\sqrt{s}$  [GeV] for  $O_{tB}$  in the helicity, beamline and off-diagonal bases. The solid curves are for the SM expectation and the dashed curves are for  $C_{tB}v^2/\Lambda^2 = 0.02$ .



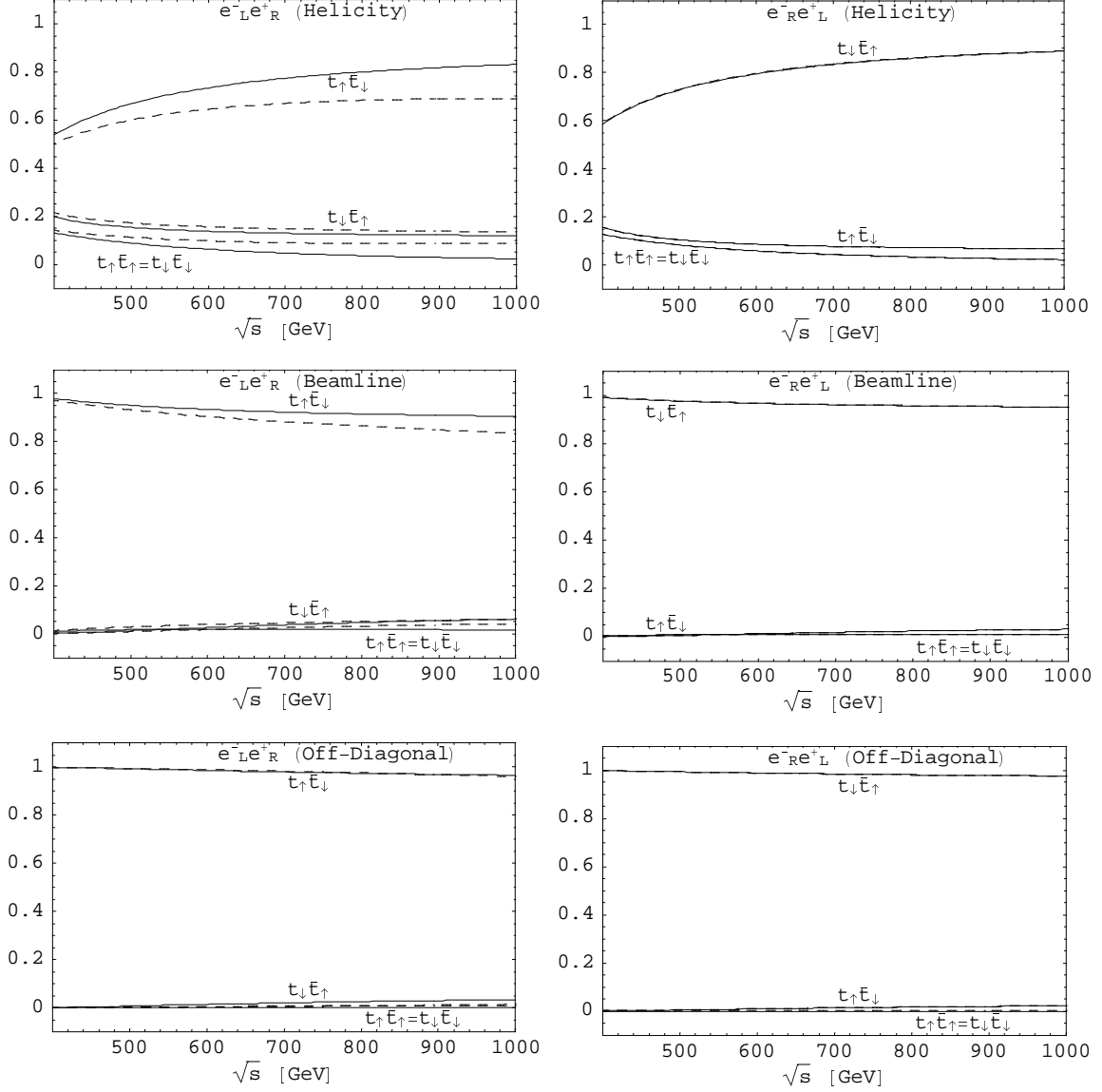


Figure 4: The fraction of top-quark pair production versus the  $e^+e^-$  c. m. energy  $\sqrt{s}$  [GeV] for  $O_{tW\phi}$  in the helicity, beamline and off-diagonal bases. The solid curves are for the SM expectation and the dashed curves are for  $C_{tW\phi}v^2/\Lambda^2 = 0.02$ .

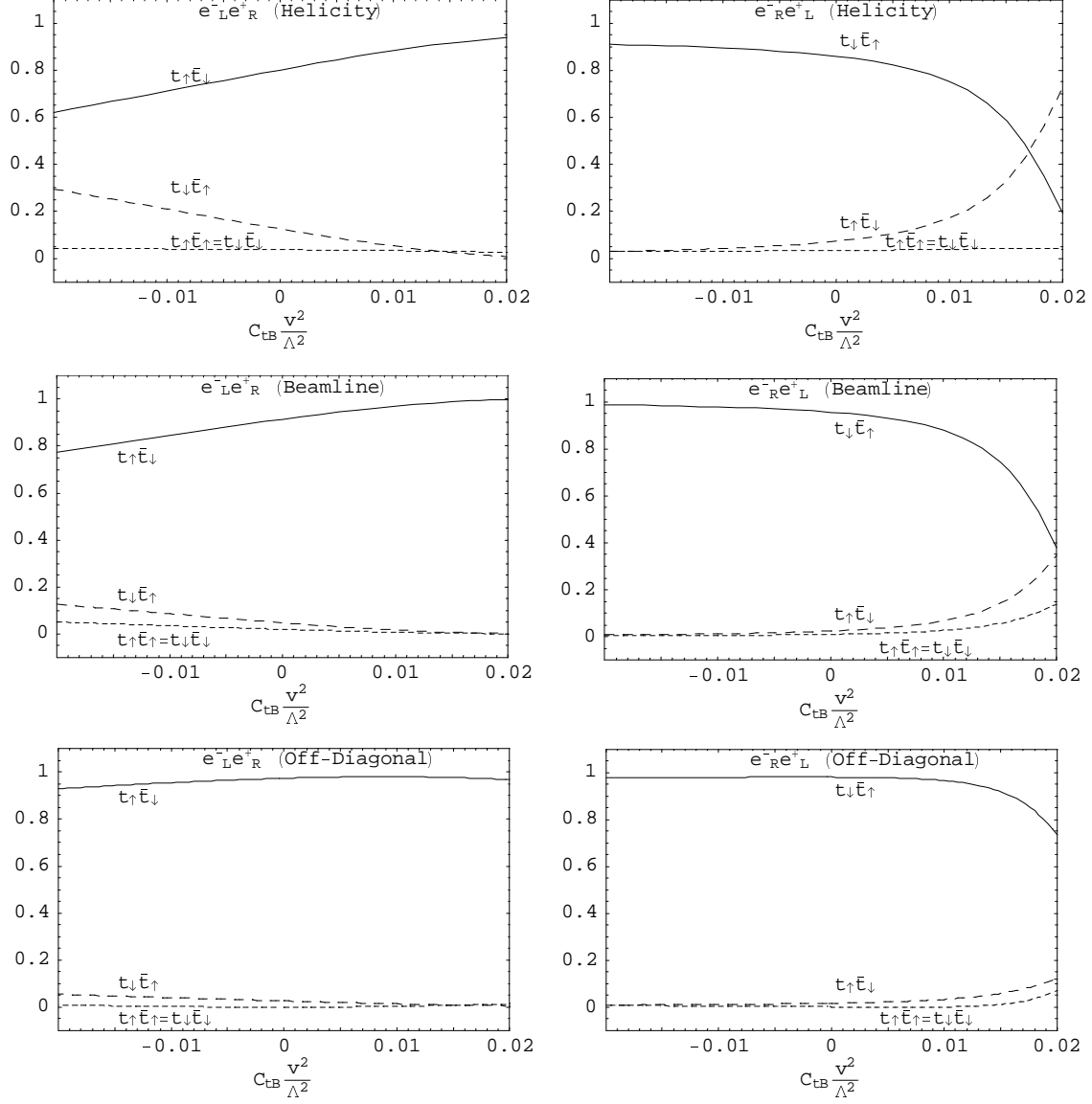


Figure 5: The fraction of top-quark pair production versus the couplings for  $O_{tB}$ ,  $C_{tB}v^2/\Lambda^2$  and  $\sqrt{s} = 800$  GeV in the helicity, beamline and off-diagonal bases .

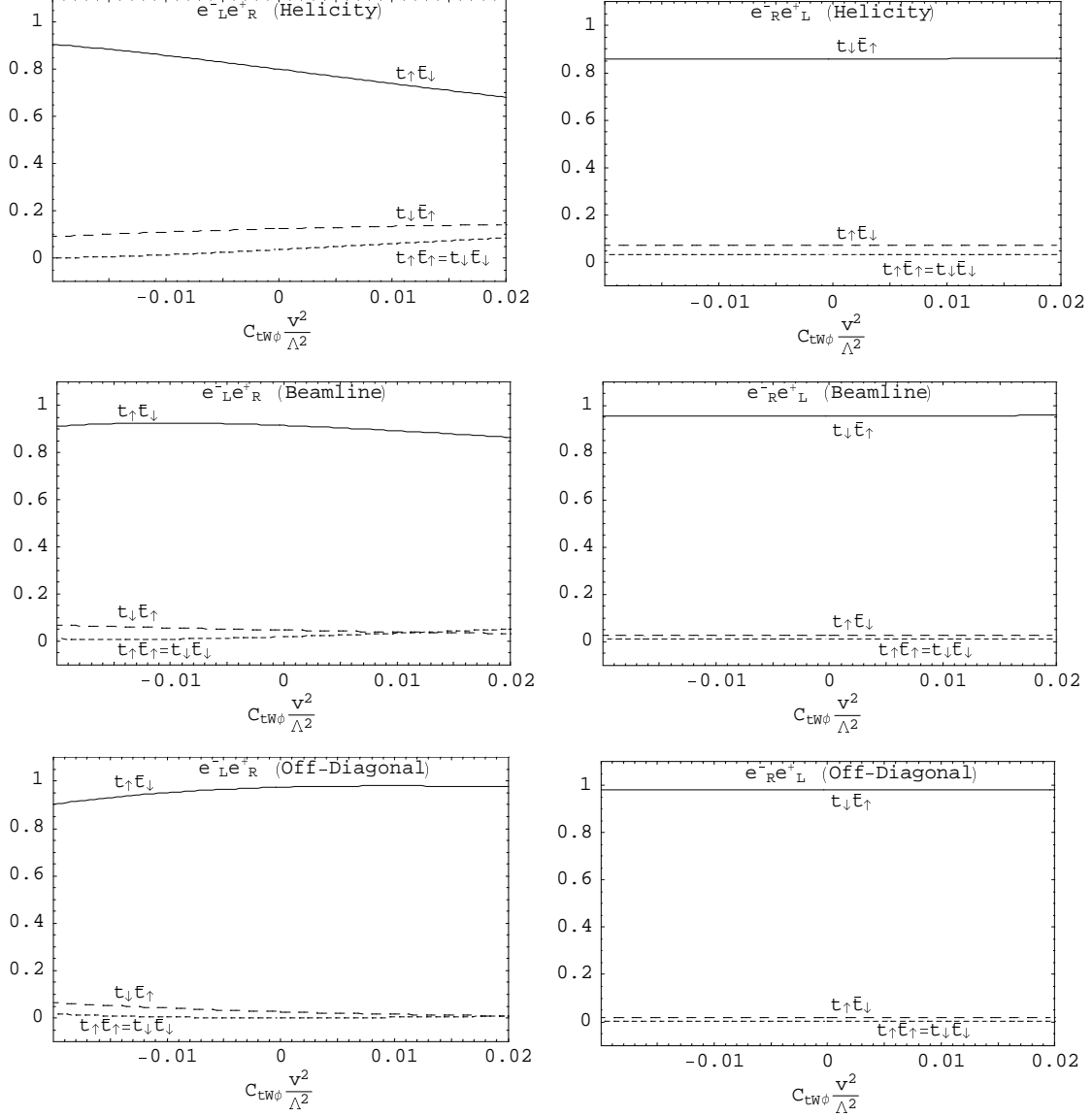


Figure 6: The fraction of top-quark pair production versus the couplings for  $O_{tW\phi}$ ,  $C_{tW\phi} v^2 / \Lambda^2$  and  $\sqrt{s} = 800$  GeV in the helicity, beamline and off-diagonal bases .

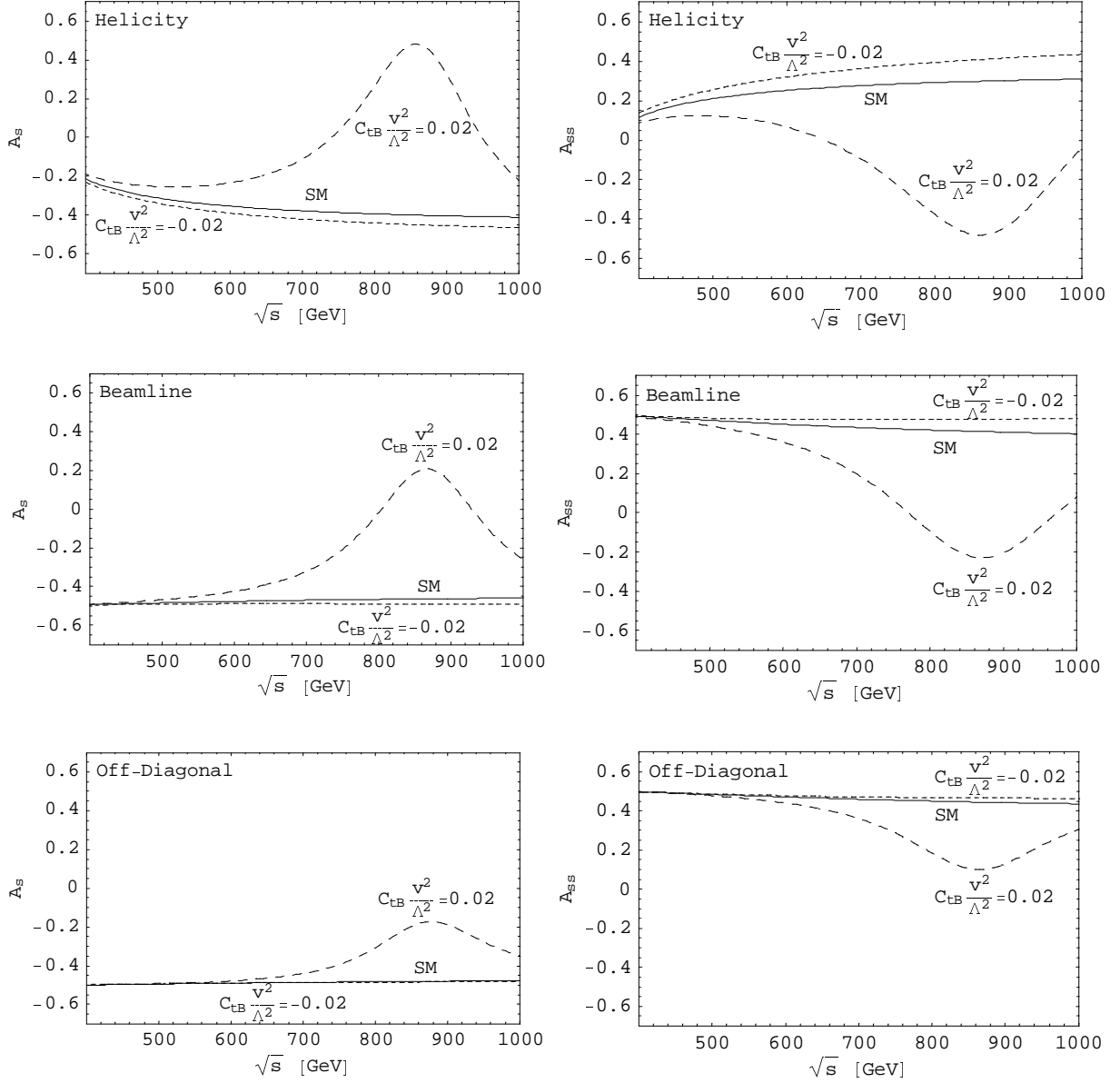


Figure 7: The spin asymmetry  $A_s$  and spin-spin asymmetry  $A_{ss}$  versus the  $e^+e^-$  c. m. energy for  $O_{tB}$  in the helicity, beamline and off-diagonal bases for right-hand polarized electron beam.

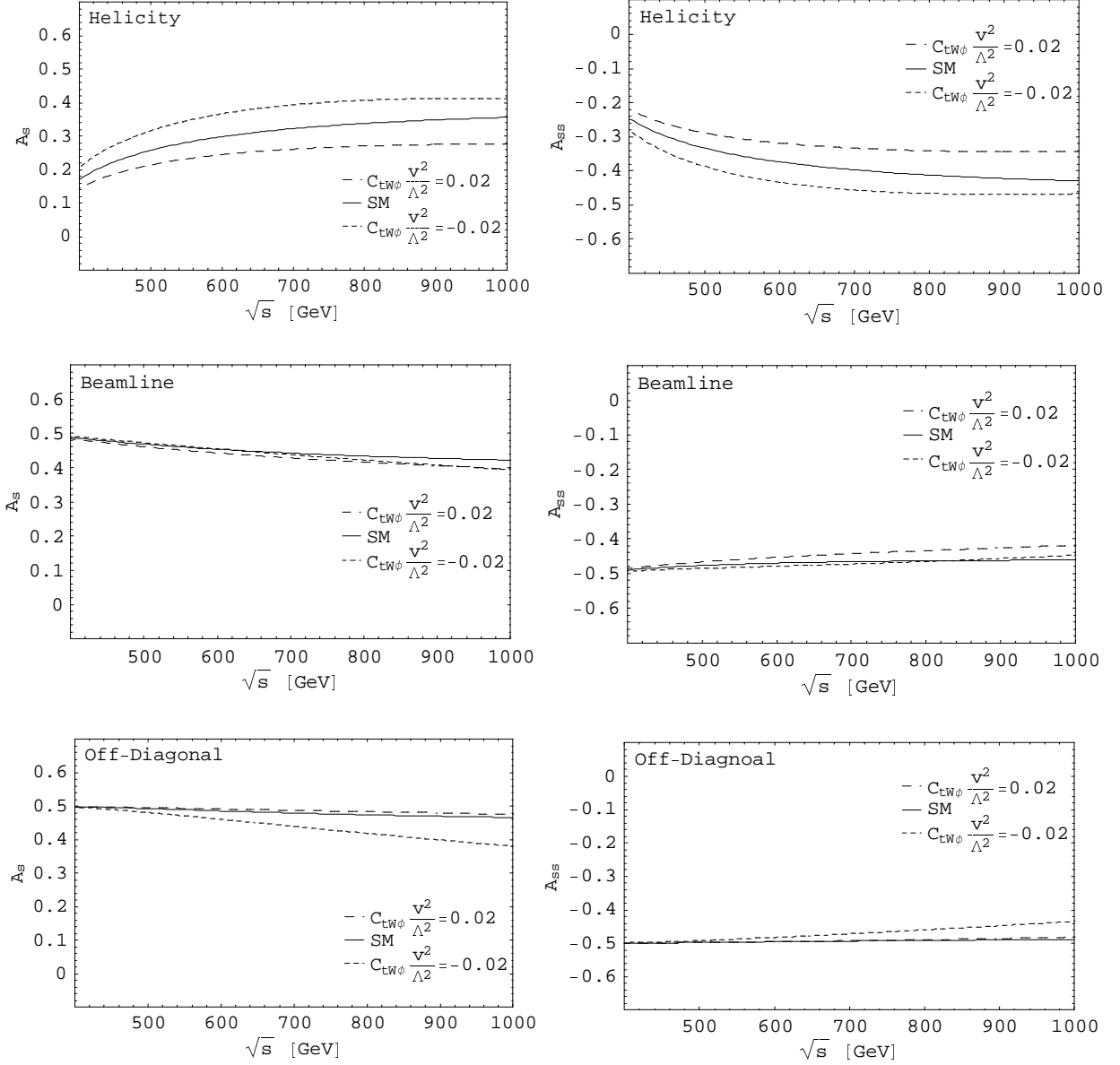


Figure 8: The spin asymmetry  $A_s$  and spin-spin asymmetry  $A_{ss}$  versus the  $e^+e^-$  c.m. energy for  $O_{tW\phi}$  in the helicity, beamline and off-diagonal bases for left-hand polarized electron beam.

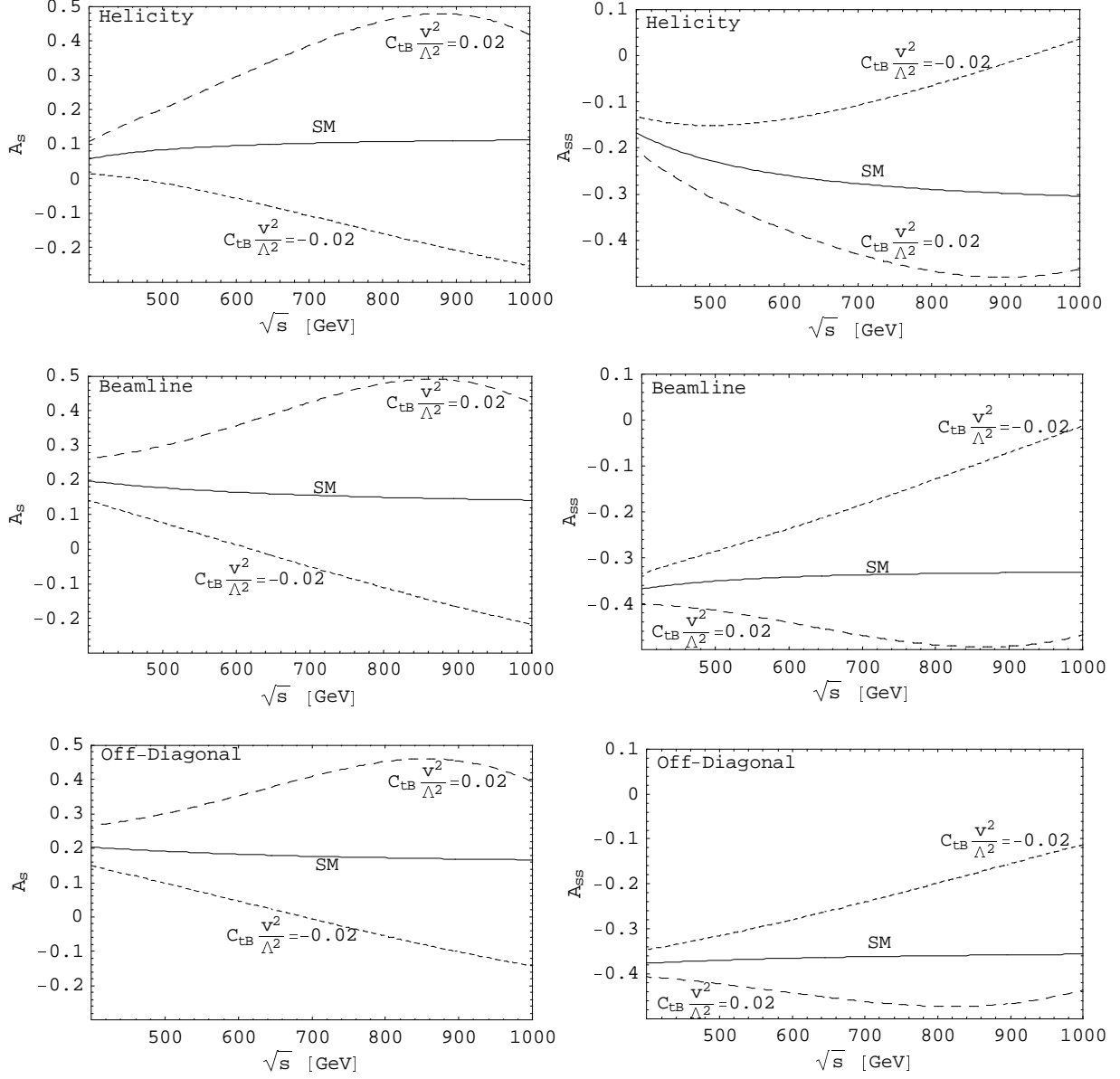


Figure 9: The spin asymmetry  $A_s$  and spin-spin asymmetry  $A_{ss}$  versus the  $e^+e^-$  c. m. energy for  $O_{tB}$  in the helicity, beamline and off-diagonal bases for unpolarized beam.

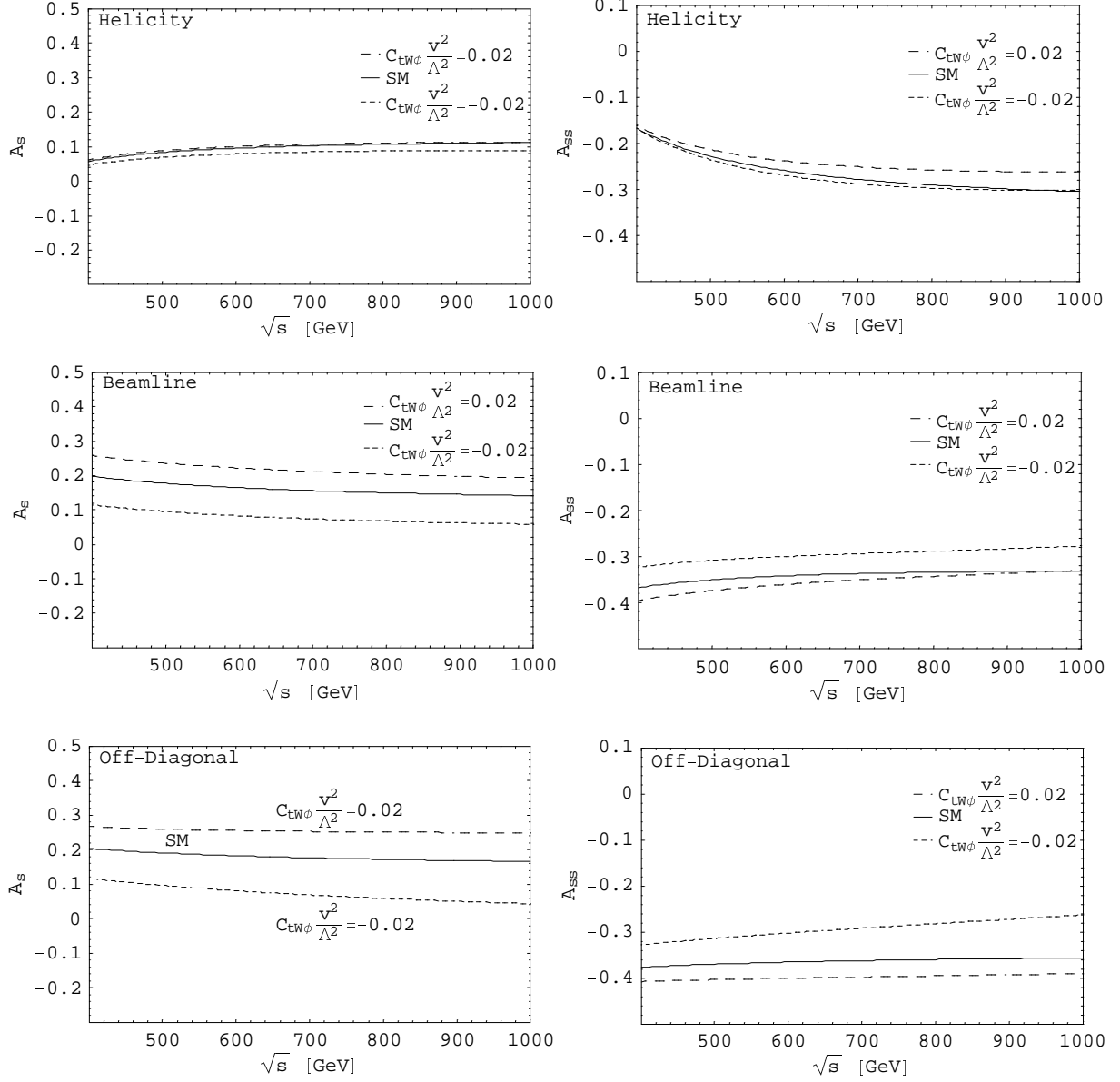


Figure 10: The spin asymmetry  $A_s$  and spin-spin asymmetry  $A_{ss}$  versus the  $e^+e^-$  c. m. energy for  $O_{tW\phi}$  in the helicity, beamline and off-diagonal bases for unpolarized beam.